Phenanthroimidazole dimers: structure and free radical reactivity; piezochromism, thermochromism, and photochromism

Yuehui Zhou, W.E. Baker, P.M. Kazmaier, and E. Buncel

Abstract: A series of 2-phenyl phenanthroimidazole dimers was synthesized by means of a two-phase preparative method, which allowed their isolation in pure form. Definitive proof of structure was obtained by means of ^{1}H and ^{13}C NMR spectroscopy; five of the six possible structural isomers of the dimer could thus be eliminated. The dimers exhibited thermochromic and piezochromic behavior, but not photochromic. The colored species were shown to be free radicals formed on dissociation of the dimers; this was confirmed through ESR measurements. The electronic absorption spectra of the radicals were influenced by substituents on the phenyl ring. The UV–VIS measurements allowed the evaluation of the dimer–radical equilibrium constants, which were also found to be dependent on substituents on the phenyl ring.

Key words: phenanthroimidazole dimers, free radical equilibrium, piezochromism, thermochromism, photochromism.

Résumé : Faisant appel à une méthode de synthèse en deux phases qui permet d'isoler les produits à l'état pur, on a synthétisé une série de dimères de la 2-phénylphénanthroimidazole. On a obtenu des preuves irréfutables de structure grâce à la spectroscopie RMN du ^{1}H et du ^{13}C; on a ainsi pu éliminer cinq des six structures isomères possibles du dimère. Les dimères présentent un comportement thermochromique et piézochromique, mais pas photochromique. Il a été démontré que les espèces colorées proviennent de radicaux libres formés lors de la dissociation des dimères; cette conclusion a été confirmée par des mesures RPE. Les spectres d'absorption électronique des radicaux sont influencés par les substituants présents sur les noyaux phényles. Les mesures UV–VIS ont permis d'évaluer les constantes d'équilibre dimère–radical; on a trouvé que celles-ci dépendent des substituants présents sur le noyau phényle.

Mots clés : dimères de la phénanthroimidazole, équilibre de radicaux libres, piézochromie, thermochromie, photochromie.

[Traduit par la rédaction]

Introduction

Nitrogen-containing heterocyclic compounds play an important role in many biological systems (1). It is known that certain dimeric nitrogen-containing heterocyclic compounds such as dimeric NAD (*N*-benzyldihydronicotinamide) are involved in some biological redox processes (2). On the other hand, triphenylimidazole dimers have also attracted attention because of the sensitivity of these compounds to light and heat, as well as to pressure. Hayashi and Maeda (3) observed that, upon oxidation with potassium ferricyanide in ethanolic solution, triphenylimidazole (**1**) gave rise to a violet color; the color then disappeared rapidly. The oxidation product was obtained as a pale violet-colored powder, which turned deep violet in solution under UV irradiation. The authors suggested (3) that the colored species was a free radical, and soon afterwards EPR evidence for the existence of the radical was presented (4).

It is now known that the oxidation product is a piezochromic dimer, which transforms to the photochromic dimer on dissolution in a solvent. In solution the photochromic dimer exists in a photostationary equilibrium with its radical form.

Radical stability in these systems has been investigated by a number of workers with respect to the influence of substituents (5). It was found that an electron-donating group on the phenyl ring will shift the photostationary state to the radical form. Interestingly, on replacing 1,4,5-triphenylimidazole by phenanthro[9,10-*d*]imidazole, so that the conjugation system is extended, the characteristics of the dimer changed dramatically. The electronic absorption of the radical form of the phenanthroimidazole dimers is shifted to longer wavelength (~600 nm) so that the solution appears blue or green, whereas the triphenylimidazole dimer solution is violet. Moreover, the dissociation of the phenanthroimidazole dimers becomes a thermal process and irradiation is no longer necessary. Various papers and patents have described the application of triphenylimidazole dimers in silver-free photographic processes (6); their application as initiators in polymerization has also been investigated (7). However, relatively few papers have elucidated problems inherent in the synthesis and characterization of the phenanthroimidazole dimer system (8). We

Received January 8, 1998.

This paper is dedicated to Professor Erwin Buncel in recognition of his contributions to Canadian chemistry.

Y. Zhou, W.E. Baker, and E. Buncel.[1] Department of Chemistry, Queen's University, Kingston, ON K7L 3N6, Canada.
P.M. Kazmaier. Xerox Research Center of Canada, Mississauga, ON L5K 2L1, Canada.

[1] Author to whom correspondence may be addressed. Telephone: (613) 545-2616. Fax: (613) 545-6669. E-mail: buncele@chem.queensu.ca

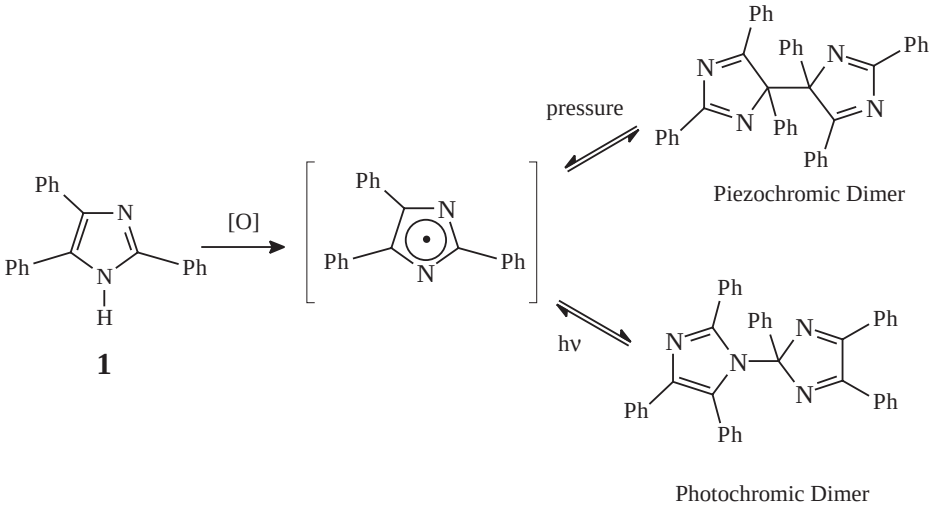

1

Scheme 1.

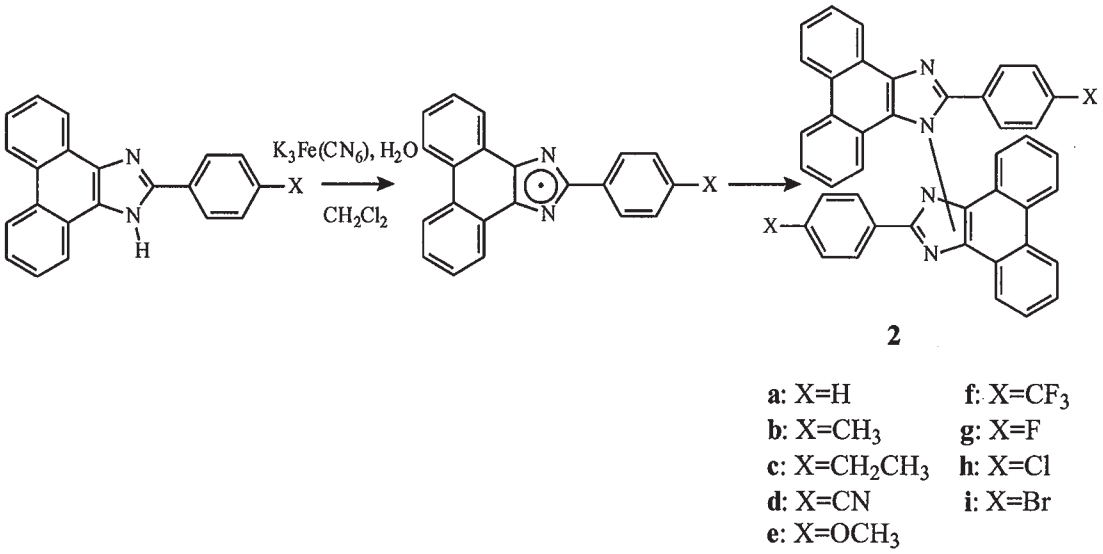

2

a: X=H
b: X=CH_3
c: X=CH_2CH_3
d: X=CN
e: X=OCH_3
f: X=CF_3
g: X=F
h: X=Cl
i: X=Br

report here our results concerning the synthesis and characterization of phenanthroimidazole dimers **2a–i**, using the oxidative synthesis method shown in Scheme 1. Compounds **2c**, **2d**, **2f**, **2g**, and **2i** have not been reported previously. Some comparisons are also made with corresponding dimer systems derived from triphenylimidazole (lophine), **1**. The original purpose of this work was to devise pressure- and sheer-sensitive dye molecules that could be used as sensors in polymer processing (9*a–d*)]; this is an extension of our studies on thermochromic and photochromic dye molecules and other photoactive pigments (9*e–r*).

Results and discussion

Synthesis

The synthesis of phenanthroimidazole dimers by the literature method used in the synthesis of triphenylimidazole dimers (10, 11), i.e., addition of an aqueous solution of potassium ferricyanide to a cold solution of the imidazole in ethanolic potassium hydroxide, proved to be unsuitable in the present work because of precipitation of reactants and isolation of impure products due to decomposition. In our experience, only dimer **2a** could be synthesized in pure form by the method used in the synthesis of triphenylimidazole dimers, probably because of its lower solubility in organic solvents, thus retarding decomposition. Coincidentally, this compound was the only one whose structure was fully elucidated by Sakaino et al. (8*a*).

Oxidation with potassium ferricyanide is of common use in organic synthesis, especially in oxidative coupling of phenols (12) and of amines (13), but, importantly, in both cases two-phase reaction conditions were used: inorganic reactant dissolved in water and the organic reactant in methylene chloride. A two-phase system (water–benzene) was used previously by Cescon et al. (5*a*) in the synthesis of triarylimidazole dimers and has been successfully applied to the synthesis of phenanthroimidazole dimers in the present work. The dimer product could be obtained in crystalline form from the organic phase after most of the solvent was evaporated; these products gave unambiguous NMR spectra. Dimer **2e** is an exception, since this gave the correct molecular peak corresponding to the dimer in the mass spectrum but failed to give a definitive NMR

Fig. 1. ^{13}C NMR spectra of representative phenanthroimidazole dimers **2a**, **2g**, and **2h**.

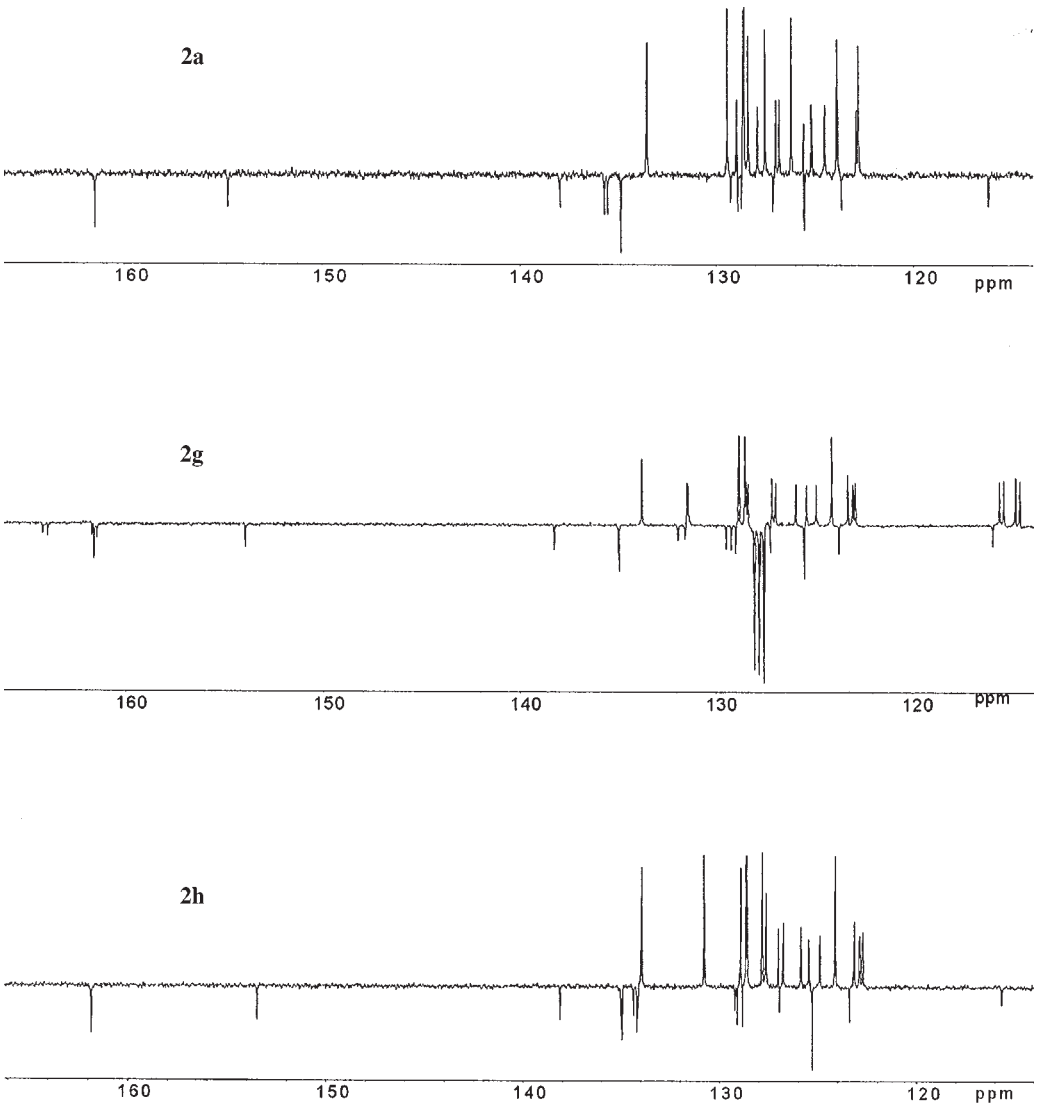

spectrum, probably because of decomposition, as indicated by the color change of the $CDCl_3$ solution. The other dimers were relatively more stable in $CDCl_3$ and allowed definitive characterization by NMR.

Structure elucidation by NMR

Triarylimidazole dimers can, in principle, exist in six structurally different isomeric forms (11). Since our work entailed a modified literature method, the structure suggested by Sakaino et al. (8*a*) for the phenanthroimidazole dimers in their work cannot be taken for granted in the case of dimers **2a–i**. Structure elucidation in the present work was based mainly on the use of NMR spectroscopy. Structures **5** and **6** can readily be excluded because of their symmetry, which would lead to a smaller number of signals of aromatic carbons than actually observed in the ^{13}C NMR spectra. Structures **7** and **8** could also be excluded, for the opposite reason, i.e., lower symmetry, which should give rise to more signals of aromatic carbons than actually observed in the ^{13}C NMR spectra. Only structures **3** and **4** satisfy the requirement of the observed number of ^{13}C NMR signals: 16 for the protonated aromatic carbons and 15 for nonprotonated aromatic carbons in the case of *para*-substituted dimers **2b–d**, **2h**, and **2i**. For the unsubstituted dimer **2a** the number of signals for protonated aromatic carbons is 18 and for nonprotonated aromatic carbons 13. However, due to overlap only 17 distinct signals were observed. In the case of the *p*-fluoro-substituted dimer **2g**, due to coupling between ^{19}F and ^{13}C (J_{CF} = 249.1 Hz, 247.7 Hz; $^1J_{CF}$ = 22.0 Hz, 21.9 Hz; $^2J_{CF}$ = 8.5 Hz, 8.3 Hz; $^3J_{CF}$ = 3.1 Hz, 3.0 Hz) the number of signals for protonated aromatic carbons increased to 20 and for nonprotonated aromatic carbons to 19 (Fig. 1). For **2f**, on the other hand, the three fluorines of the trifluoromethyl group split the signals of the vicinal carbons of the phenyl ring to a quartet ($^1J_{CF}$ = 32.5 Hz, 32.3 Hz), increasing the signal number of nonprotonated ring carbons to 21. Again, due to overlap only 15 protonated and 20 nonprotonated carbon signals were observed. The other eight signals corresponding to two quartets (J_{CF} = 272.3 Hz, 272.3 Hz) in the aromatic chemical shift region stem from the two trifluoromethyl carbons due to the deshielding and coupling with the three fluorines (Table 1).

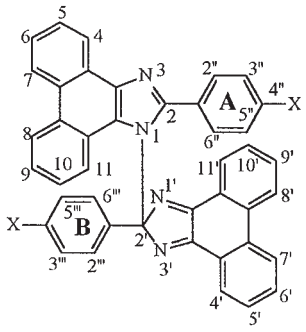

3

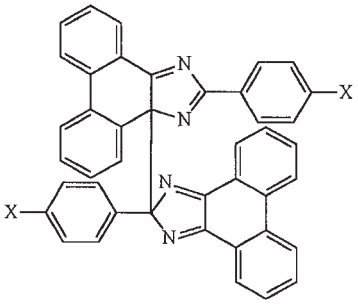

4

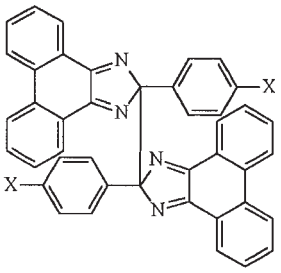

5

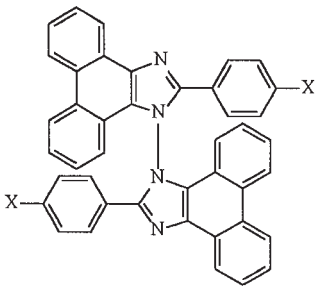

6

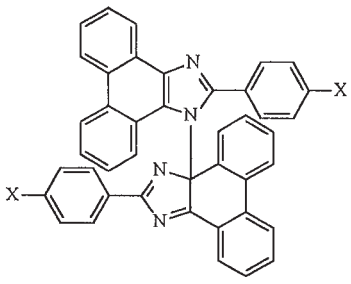

7

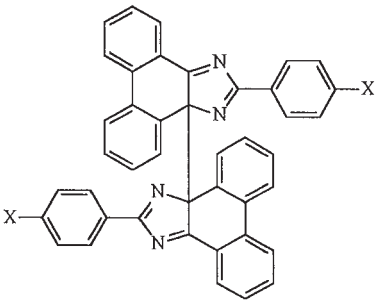

8

To distinguish between structures **3** and **4**, we have made use of the reference compounds **9**–**14** reported in the literature (8*a*, 14), which are good representatives of the half-dimer subunits. The ^{1}H NMR chemical shifts (in ppm) for the 2,6-protons on the 2-phenyl ring are as follows: <8.0 in **9**, **10**; 8.47, 8.18 in **11**; 7.50 in **12**; 7.85 in **13**; and 8.45 for **14**.

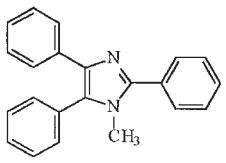

9

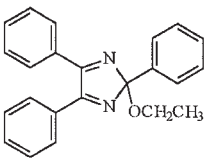

10

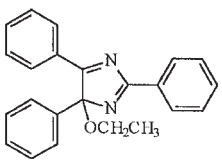

11

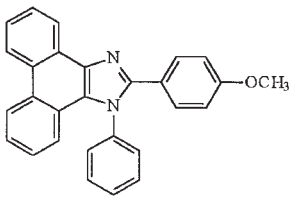

12

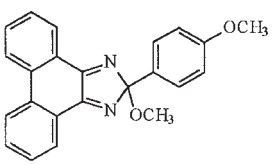

13

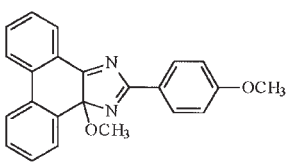

14

Table 1. Summary of ^{13}C NMR chemical shifts of ring carbons in phenanthroimidazole dimers (solvent $CDCl_3$, $CDCl_3$ + C_6D_6 (3:1 v/v) for **2g**, TMS as internal reference).

	Protonated carbons				Nonprotonated carbons			
2a	133.55	129.47	128.98	128.66	161.47	154.79	137.97	135.71
	128.61	128.43	127.94	127.55	135.55	134.89	129.28	128.92
	127.01	126.83	126.22	125.59	128.76	127.13	125.55	123.69
	125.19	124.52	123.89	122.96	116.21			
	122.81							
2b	133.39	129.36	129.11	128.72	161.20	154.93	138.87	138.01
	128.50	128.23	127.09	126.80	137.94	134.84	132.82	132.45
	126.18	125.51	125.22	124.43	129.21	128.86	128.76	127.20
	123.89	122.91	122.84	122.79	125.82	123,82	116.22	
2c	133.35	129.39	128.615	128.56	161.17	154.95	145.13	144.18
	127.92	127.08	127.03	126.80	137.92	134.81	132.91	132.53
	126.22	125.50	125.19	124.40	129.39	128.85	128.75	127.17
	123.86	122.85	122.81	122.79	125.74	123.80	116.25	
2d	134.65	132.19	131.33	130.05	162.71	152.78	140.88	139.97
	129.10	128.55	127.25	127.05	138.32	135.07	129.39	129.29
	126.36	126.22	125.60	125.39	128.90	126.74	124.93	122.94
	124.38	123.37	122.98	122.63	118.27	117.91	115.32	
2f	134.21	129.88	128.99	128.51	162.32	153.04	139.72	139.31
	127.13	126.60	126.04	125.55	138.27	135.02	131.20[a]	129.85[b]
	125.11	124.59	124.56	124.17	129.26	128.90	126.92	124.99
	123.27	122.92	122.75		123.19	115.57		115.57
2g	133.79	131.43[c]	128.82	128.52	162.94[g]	162.69[h]	161.61	153.97
	128.41[d]	127.14	126.97	125.92	138.26	134.96	131.94[i]	131.57[j]
	125.38	124.88	124.10	123.28	129.48	129.21	128.99	127.24
	123.02	122.91	115.44[e]	114.61[f]	125.50	123.74	115.88	
2h	133.98	130.80	128.94	128.67	161.83	153.50	138.13	135.03
	128.62	127.85	127.65	127.02	134.97	134.39	134.22	134.66
	126.79	125.88	125.48	124.92	129.23	129.11	128.86	126.97
	124.14	123.18	122.90	122.75	125.32	123.42	115.67	
2i	134.02	131.63	131.04	130.78	161.86	153.74	138.12	134.98
	129.01	128.68	127.89	127.05	134.76	134.61	129.20	129.14
	126.77	125.90	125.51	124.95	128.87	126.95	125.30	123.37
	124.15	123.20	122.90	122.73	123.31	122.75	155.71	

[a] Quartet, $J = 32.5$ Hz.
[b] Quartet, $J = 32.3$ Hz.
[c] Doublet, $J = 8.3$ Hz.
[d] Doublet, $J = 8.5$ Hz.
[e] Doublet, $J = 22.0$ Hz.
[f] Doublet, $J = 21.9$ Hz.
[g] Doublet, $J = 249.1$ Hz.
[h] Doublet, $J = 247.7$ Hz.
[i] Doublet, $J = 3.0$ Hz.
[j] Doublet, $J = 3.1$ Hz.

The reference compounds **9**–**14** fall into two structurally similar sets: the triaryl imidazole series **9**–**11** and the phenanthroimidazole series **12**–**14**. These structural parallels are reflected in parallel trends in the ^1H NMR chemical shifts of the 2-phenyl 2,6-protons. The COSY and ^1H NMR spectra of the synthesized dimers indicate that the resonance of the 2-phenyl 2,6-protons was lower than 8.00 ppm, the chemical shift values being <8.00 (**2a**); 7.31, 7.0 1(**2b**); 7.34, 7.05 (**2c**); 7.51, 7.19 (**2d**); 7.41, 7.25 (**2f**); 7.35, 7.06 (**2g**); 7.35, 7.05 (**2h**); and 7.28, 7.15 (**2i**), respectively (Table 2). This shows that the dimer structure must be made of two moieties that resemble the reference compounds **12** and **13**. Hence generic structure **3** is assigned to the synthesized dimers, which is consistent with the conclusions of the earlier work (8*a*). Moreover, by analysis of the COSY spectra on the dimers and the NOE results, we could make unambiguous assignment of the ^1H NMR spectra of the dimers (in the case of **2a**, only assignment for the phenanthryl rings was made) as shown in Table 2.

The assignment is made on the following basis: (*i*) the chemical shift values of protons in ring A bonded to the imidazole ring via an sp^2 carbon will be higher (further downfield) than those in the ring B bonded to the imidazole ring via an sp^3 carbon, because of more facile transmission of electronic effects in the former case. (*ii*) The protons on the asymmetric phenanthroimidazole ring at positions 4 and 11 have the same splitting pattern and integral values, but the higher chemical shift is assigned to position 11 since molecular models have shown that the proton at this position is the more "crowded."

Table 2. Assignment of ^{1}H NMR chemical shifts in structure **3** (*J* in Hz).

	3a	**3b**	**3c**	**3d**	**3f**	**3g**	**3h**	**3i**
4	8.89 (d, 7.5, 1H)	8.85 (d, 7.9, 1H)	8.85 (d, 7.9, 1H)	8.77 (d, 7.8, 1H)	8.81 (d, 7.9, 1H)	8.93 (d, 8.0, 1H)	8.81 (d, 7.9, 1H)	8.80 (d, 7.9, 1H)
5	7.71 (t, 7.4, 1H)	7.67 (t, 7.0, 1H)	7.65 (t, 7.4, 1H)	7.70 (t, 7.5, 1H)	7.70 (t, 7.3, 1H)	7.64 (t, 7.5, 1H)	7.69 (t, 7.3, 1H)	7.69 (t, 7.1, 1H)
6	7.64 (d, 6.9, 1H)	7.61 (t, 7.6, 1H)	7.59 (t, 9.0, 1H)	7.65 (d, 7.6, 1H)	7.64 (t, 7.3, 1H)	7.54 (t, 7.7, 1H)	7.62 (t, 8.0, 1H)	7.63 (t, 7.7, 1H)
7	8.69 (d, 8.1, 1H)	8.66 (d, 8.2, 1H)	8.65 (d, 7.9, 1H)	8.66 (d, 7.4, 1H)	8.67 (d, 8.2, 1H)	8.59 (d, 8.1, 1H)	8.66 (d, 8.2, 1H)	8.67 (d, 8.6, 1H)
8	8.70 (d, 8.2, 1H)	8.67 (d, 7.9, 1H)	8.65 (d, 7.9, 1H)	8.68 (d, 7.6, 1H)	8.69 (d, 7.9, 1H)	8.61 (d, 8.3, 1H)	8.68 (d, 8.1, 1H)	8.69 (d, 8.7, 1H)
9	7.49 (t, 7.8, 1H)	7.46 (t, 7.6. 1H)	7.44 (t, 7.5, 1H)	7.51 (t, 8.2, 1H)	7.50 (t, 7.6, 1H)	7.41 (t, 7.9, 1H)	7.49 (t, 7.6, 1H)	7.51 (t, 7.4, 1H)
10	7.41 (t, 7.6, 1H)	7.39 (t, 7.7, 1H)	7.36 (t, 7.6, 1H)	7.41 (t, 8.5, 1H)	7.40 (t, 7.9, 1H)	7.41 (t, 7.9, 1H)	7.41 (t, 7.5, 1H)	7.42 (t, 7.8, 1H)
11	9.37 (d, 8.4, 1H)	9.38 (d, 8.3, 1H)	9.32 (d, 8.4, 1H)	9.28 (d, 8.3, 1H)	9.30 (d, 8.3, 1H)	9.39 (d, 8.3, 1H)	9.35 (d, 8.4, 1H)	9.34 (d, 8.3, 1H)
4′(11′)	8.06 (d, 8.1, 2H)	8.09 (d, 8.1, 2H)	8.04 (d, 8.5, 2H)	8.16 (d, 8.1, 2H)	8.12 (d, 8.1, 2H)	8.02 (d, 7.7, 2H)	8.11 (d, 8.1, 2H)	8.14 (d, 8.1, 2H)
5′(10′)	7.60 (t, 7.4, 2H)	7.61 (t, 7.6, 2H)	7.30 (d, 8.0, 2H)	7.72 (t, 7.7, 2H)	7.67 (t, 7.7, 2H)	7.21 (t, 7.5, 2H)	7.65 (t, 8.2, 2H)	7.68 (t, 7.9, 2H)
6′(9′)	7.34 (t, 7.5, 2H)	7.35 (t, 7.5, 2H)	7.57 (d, 8.3, 2H)	7.45 (t, 7.5, 2H)	7.37 (t, 7.5, 2H)	7.42 (t, 7.9, 2H)	7.41 (t, 7.5, 2H)	7.44 (t, 7.7, 2H)
7′(8″)	8.03 (d, 7.7, 2H)	8.05 (d, 7.2, 2H)	8.02 (d, 8.0, 2H)	8.00 (d, 7.6, 2H)	7.96 (d, 7.5, 2H)	7.87 (d, 8.1, 2H)	8.04 (d, 7.7, 2H)	8.04 (d, 7.7, 2H)
2″(6″)		7.31 (d, 7.9, 2H)	7.34 (d, 8.0, 2H)	7.51 (d, 8.1, 2H)	7.41 (d, 8.2, 2H)	7.35 (q, 8.6, 2H)[a]	7.35 (d, 8.4, 2H)	7.28 (d, 8.7, 2H)
3″(5″)		6.90 (d, 7.8, 2H)	6.90 (d, 7.7, 2H)	7.40 (d, 8.4, 2H)	7.55 (d, 7.9, 2H)	6.69 (t, 8.7, 2H)[b]	7.10 (d, 8.5, 2H)	7.25 (d, 8.6, 2H)
2‴(6‴)		7.01 (d, 8.3, 2H)	7.05 (d, 8.2, 2H)	7.19 (d, 8.6, 2H)	7.25 (d, 8.6, 2H)	7.06 (q, 8.9, 2H)[c]	7.05 (d, 8.8, 2H)	7.15 (d, 8.6, 2H)
3‴(5‴)		6.81 (d, 8.2, 2H)	6.83 (d, 8.1, 2H)	7.30 (d, 8.6, 2H)	7.31 (d, 8.6, 2H)	6.57 (t, 8.6, 2H)[d]	6.99 (d, 8.8, 2H)	6.98 (d, 8.6, 2H)
		2.11 (s, CH_3)	2.41 (q, 8.0, CH_2)					
		2.09 (s, CH_3)	2.39 (q, 8.0, CH_2)					
			1.02 (t, 7.2, CH_3)					
			0.99 (t, 7.3, CH_3)					

[a] $J_{HF(meta)}$ = 5.4 Hz.
[b] $J_{HF(ortho)}$ = 8.7 Hz.
[c] $J_{HF(meta)}$ = 5.1 Hz.
[d] $J_{HF(ortho)}$ = 8.6 Hz.

Fig. 2. (*a*) Spectra of dimer **2h** in benzene (8.55×10^{-5} M) after UV irradiation for 20 s at 25°C, solid line: before irradiation; dotted line: after irradiation. (*b*) Spectra of lophine dimer in benzene (9.15×10^{-5} M) after UV irradiation for 20 s at 25°C, solid line: before irradiation; dotted line, after irradiation.

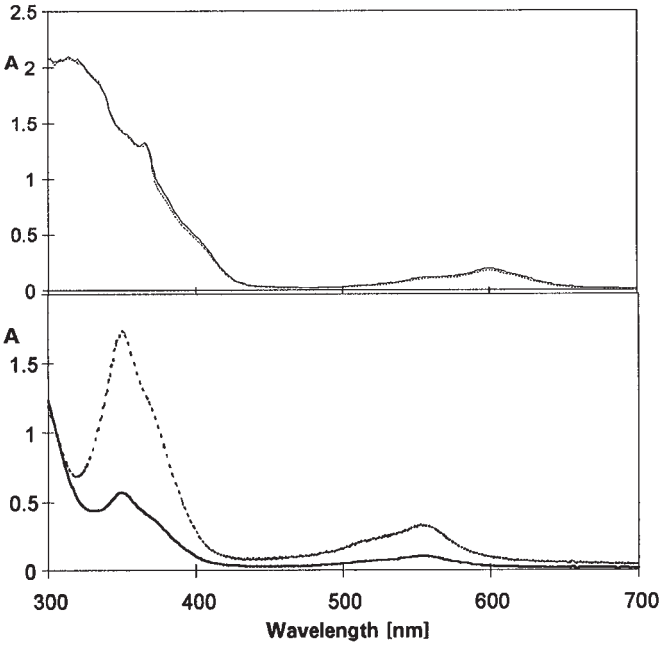

This crowding is also found in the optimized structure of dimer **2e** by the AM1 computational method.[2] Other cases have been recorded in the literature where "crowded" protons in aromatic compounds were found to have abnormally high chemical shifts (15). (*iii*) The protons at positions 4′(11′) and 7′(8′) on the symmetric phenanthroimidazole ring have the same splitting pattern and integral value, and the higher chemical shift value is assigned to position 4′(11′) due to proximity of the nitrogen in the imidazole ring. (4). Other assignments are based on results of COSY experiments with each dimer.

Features (*i*) and (*ii*) have been confirmed by means of an NOE experiment with dimer **2b**, the results of which show a strong Overhauser effect between protons having chemical shifts 9.38 and 7.01. These two values have been assigned to the protons at positions 11 and 6‴(2‴). The results of the AM1 optimization on dimer **2b** also reveal that the spatial distance between positions 11 and 6‴(2‴) is 2.81 Å,[2] which falls in the effective range of Overhauser effects (16). In the work of Sakaino et al. (8*a*), a chemical shift of 9.3 was also assigned to the proton at position 11 of dimer **2a**, though definitive proof for the assignment was not given.[3]

[2] S. Chen, Y. Zhou, and E. Buncel. Unpublished results.

[3] It has been pointed out by a referee that one can distinguish between structures **3** and **4** on the basis of symmetry. Structure **4** has a stereogenic centre at the dimer linkage to the top imidazole ring. Hence the lower phenanthroimidazole ring system does not have symmetry and will have the same carbon count in the ^{13}C NMR as the lower ring in **7**, which leaves the generic structure **3** as the only possible one. We thank the referee for this observation, which complements the structural assignment made on the basis of the experimental NMR evidence.

Fig. 3. (*a*) Spectra of dimer **2h** in benzene (8.67×10^{-5} M) on heating from 25°C (solid line) to 60°C (dotted line). (*b*) Spectra of lophine dimer in benzene (9.15×10^{-5} M) on heating from 25°C (solid line) to 60°C (dotted line).

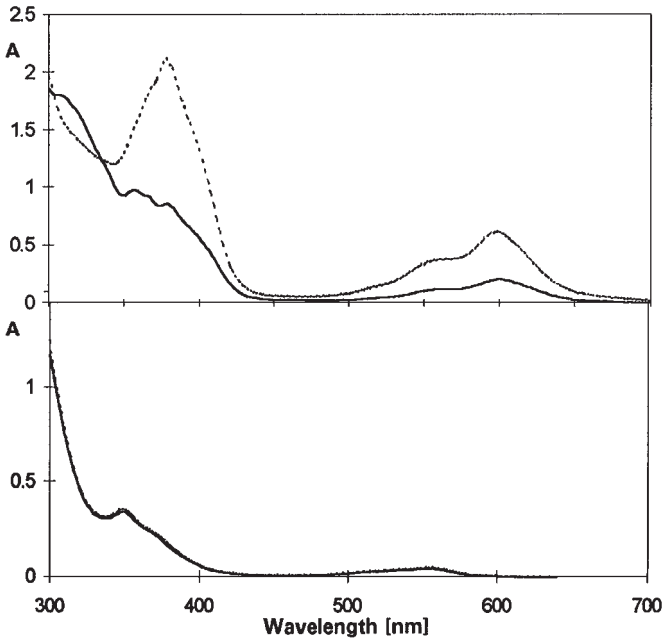

Photochromism

The synthesized phenanthroimidazole dimers are not photosensitive at room temperature. Thus the absorbance of the dimer solution in benzene remains constant under irradiation (Fig. 2*a*); in contrast the absorbance of the solution of lophine dimer in benzene increased 2–3 fold under identical irradiation conditions (Fig. 2*b*). Figure 2*a* shows the constant absorbance of the solution of dimer **2h** in benzene at 25°C after UV irradiation for 20 s. All other synthesized phenanthroimidazole dimers behave similarly to dimer **2h** toward UV irradiation.

Thermochromism

In contrast to the lack of an effect of UV irradiation on spectra in the phenanthroimidazole dimer series, the absorbance of the dimer solutions in benzene increased 2–3 fold when the temperature of the solutions was raised from 25°C to 60°C (Fig. 3*a*); on cooling the color faded again. The process of color development on heating and the subsequent fading of color on cooling could be repeated a number of times. However, a gradual decomposition took place on standing at a given temperature. This color fading followed a first-order process, but it was not possible to identify the products of decomposition. The triphenylimidazole dimers, in contrast, show little or no change in their UV–VIS spectra on heating (Fig. 3*b*), even though literature reports claim these compounds to also be thermochromic (10, 17).

Piezochromism

We have found that all synthesized phenanthroimidazole dimers are pressure sensitive: the originally brown or yellow crystals turned green or bluish green upon grinding. The colored ground dimers could be pressed to a transparent disc with potassium bromide and the absorption in the visible range

Fig. 4. Representative UV–vis spectra of dimers **2e** and **2h** in KBr disc after grinding and pressurization.

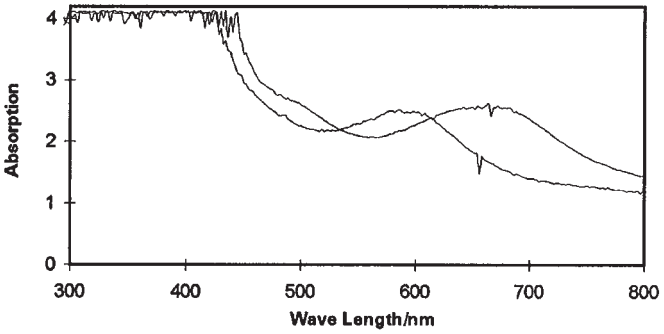

Table 3. Spectral characteristics of dimers in benzene solution and in KBr disc.

	λ_{max} (nm)	
	Benzene	KBr
2a	584	586
2b	612	594
2c	612	580
2d	552	552
2e	648	654
2f	570	570
2g	582	574
2h	600	588
2i	604	604

recorded (Fig. 4). After several days the color formed through grinding and pressurization faded. Interestingly, it was found that spectra recorded in this way displayed a bathochromic shift with electron-donating substituents such as OCH_3 and CH_3, similar to the observation with the benzene solutions of these dimers (Table 3).

It seems plausible that the observed color development on grinding and pressurization is due to dissociation of the dimers to free radicals, although it is not clear whether the dissociation is brought about by crystal deformation or rupture through external pressure, or as a result of a thermal effect from mechanical grinding. Both factors have been reported to cause color change through structural changes (18). In general, one expects formation of two radicals from a dimer to be accompanied by an increase in molecular volume, but in the present system the reverse situation may obtain since the radicals will be essentially planar and capable of stacking, which is clearly not the case with the dimer as shown by molecular models and AM1 calculations. The experiments described below prove conclusively that the colored species formed from the dimers are indeed free radicals.

Dimer–radical equilibrium

It was possible to investigate the dimer–radical thermal equilibrium for the phenanthroimidazole dimers and to determine the molar extinction coefficient as well as the equilibrium constant for formation of the radical species by means of the following derivations.

Consider the dissociation of the dimer to its radical form:

Table 4. Equilibrium constants and molar extinction coefficients calculated from the slope and intercept of A versus $[D]_o/A$ plots of dimer solutions in benzene at 25°C, and the fraction of dissociation, $\alpha = K^{1/2}$.

	$-\log K$	$10^{-3}\varepsilon$	$10^{3}\alpha$
2a	5.99±0.06	8.87±0.64	1.01±0.07
2b	5.19±0.04	10.10±0.06	2.58±0.08
2c	5.35±0.04	11.54±0.41	2.13±0.09
2g	5.88±0.07	13.43±1.11	1.16±0.10
2h	5.88±0.02	10.72±0.24	1.16±0.03
2i	5.84±0.04	8.95±0.49	1.21±0.06

Table 5. Influence of substituents (19) on λ_{max} of free radicals and on the dimer–radical dissociation constants in benzene at 25°C.

	σ_{para}	λ_{max} (nm)	$-\log K$
2e (OCH_3)	–0.27	648	
2b (CH_3)	–0.17	612	5.19
2c (CH_2CH_3)	–0.15	612	5.35
2a (H)	0	584	5.99
2g (F)	0.06	582	5.88
2h (Cl)	0.23	600	5.88
2i (Br)	0.23	604	
2f (CF_3)	0.54	570	[a]
2d (CN)	0.66	552	[a]

[a] K values too small to be measured accurately.

$$D \rightleftharpoons R + R$$

where D stands for the dimer and R for the radical formed from the dimer on dissociation. The equilibrium constant is given by

$$K = \frac{[R]^2}{4[D]} = \frac{[R]^2}{4[D]_0 - 2[R]}$$

where [D] and [R] refer to the equilibrium concentrations while $[D]_0$ is the initial dimer concentration. If the Lambert–Beer law is valid and the radical species is responsible for the color formation, then $[R] = A/\varepsilon l$, where A is absorbance, ε the molar extinction coefficient, and l, the light pathlength, equals 1. Hence

$$K = \frac{(A/\varepsilon)^2}{4[D]_0 - 2(A/\varepsilon)}$$

$$A = 4K\varepsilon^2 \frac{[D]_0}{A} - 2K\varepsilon = a\frac{[D]_0}{A} - b$$

It follows that a plot of A against $[D]_0/A$ will be linear with slope $a(= 4K\varepsilon^2)$ and intercept $b(= 2K\varepsilon)$. The molar extinction coefficient ε and equilibrium constant K can then be obtained: $\varepsilon = a/2b$ and $K = b^2/a$. The degree of dissociation is given by $\alpha = K^{1/2}$ (where $\alpha << 1$).

In Fig. 5 is shown the relevant plot of A vs. $[D]_o/A$ for the various substituted dimers and it is seen that satisfactory linearity is obtained. The resulting values of K, ε, and α are given in Table 4. Importantly, the results show that the fraction of dissociation of the phenanthroimidazole dimers to radical is of the order of 10^{-3}. This is consistent with the fact that the NMR spectra of the dimers appear to be free of paramagnetic

Fig. 5. Plot of A versus $[D_0]/A$ for dimer solutions in benzene at 25°C (correlation r^2: **2a** l, l; **2b** 0.9999, 0.9992; **2c** 0.9999, 0.9995; **2g** 0.9999, 0.9997; **2h** 0.9999, 0.9998; **2i** 0.9999, 0.9998).

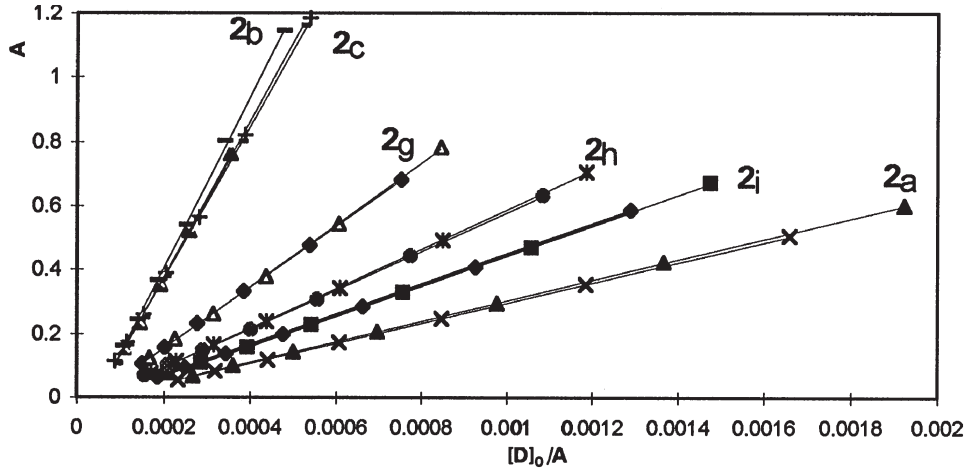

Fig. 6. (*a*) Hyperfine ESR spectrum of dimer **2b** in benzene (1.873×10^{-4} M) at room temperature, scale: 1.52 G/cm, scan range 25 G. (*b*) Hyperfine ESR spectrum of 2-*p*-methylphenyl-4,5-diphenylimadazole dimer in benzene (9.15×10^{-5} M) at room temperature, scale: 3.05 G/cm, scan range 50 G.

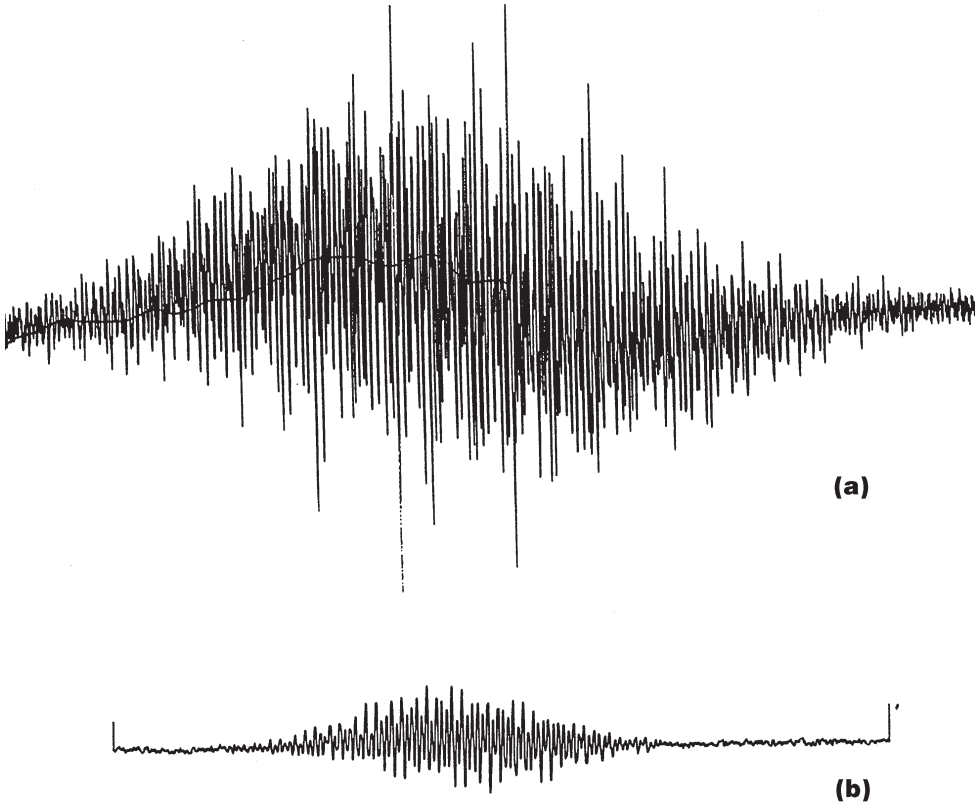

interference. In that regard, it is interesting that Maeda and Hayashi (10) reported a degree of dissociation, $\alpha = 0.3$, for triphenylimidazole dimers, although one might have expected α to be smaller for triphenylimidazole dimers than for phenanthroimidazole dimers.

The results in Table 5 indicate that the dimer–radical equilibrium constants increase as the *para* substituents on the 2-phenyl ring of the dimers become more electron donating (Table 5). This is consistent with the trend that electron-donating substituents stabilize the radicals, as was also found for dissociation of triphenylimidazole dimers (5). The halogenated phenanthroimidazole dimers do not show a clear trend, given the experimental error in measurement of K, though the λ_{max} values exhibit a reverse trend relative to the electron-donating substituents. The strong electron-withdrawing trifluoromethyl and cyano substituents both exhibit a hypsochromic effect on λ_{max} and decreased dissociation constants, which were in fact too small to be measured accurately.

Fig. 7. ESR spectra of lophine dimer in benzene (8.53×10^{-5} M) at room temperature, scale: 1.22 G/cm, scan range 20 G; (*a*) before irradiation; (*b*) after irradiation.

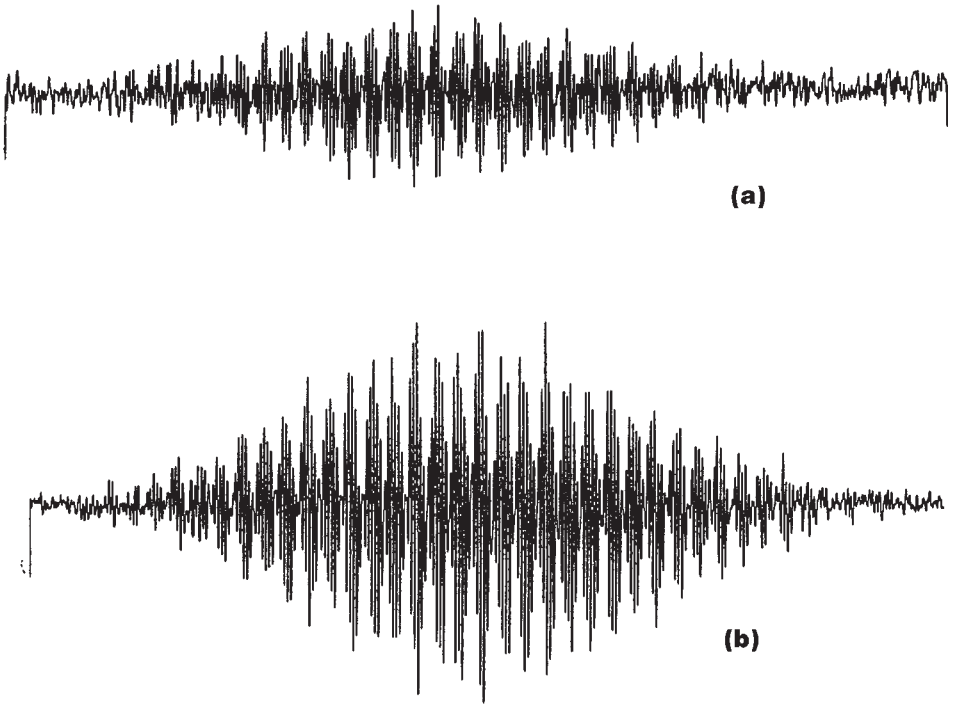

Fig. 8. ESR signals of dimer **2b** in benzene (1.173×10^{-4} M) at room temperature (left, signal gain 5×10^4) and at 65°C (right, signal gain 2×10^3), scale: 19.53 G/cm, scan range 500 G).

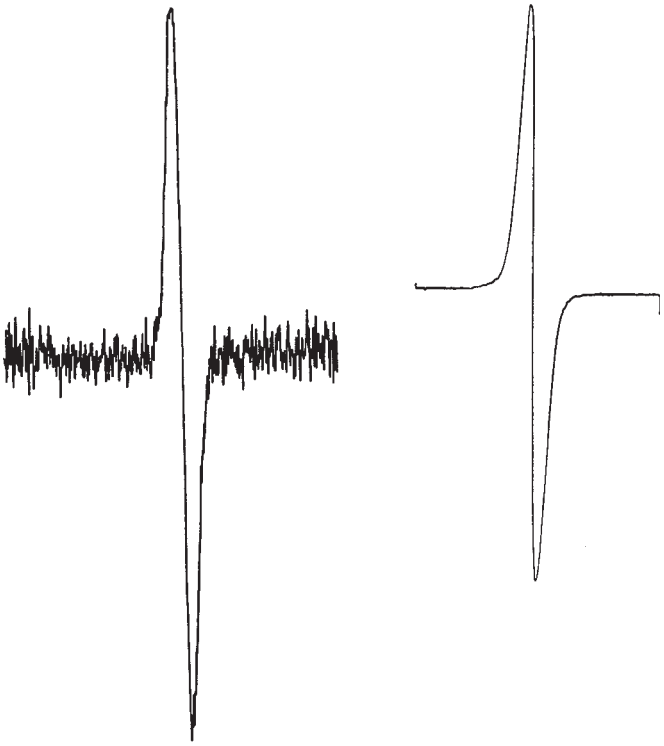

Fig. 9. ESR signals of dimer **2b** solid sample (weak) and its ground powder (strong) at room temperature, scale: 15.62 G/cm, scan range 400 G.

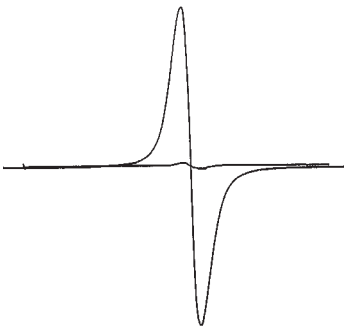

ESR spectra

Several studies have reported on the ESR hyperfine structure of the free radical derived from the lophine dimer (20, 21) and the radical anion derived from lophine (22). It was found that the free radical of the lophine dimer has spin density distributed in all three phenyl rings even though these are twisted out of the plane of the imidazole ring and also with respect to one another (21). One would expect that in the free radical derived from the phenanthroimidazole dimer the spin density would be more delocalized because of the extended conjugation, leading to more complex ESR hyperfine structure. We have, indeed, obtained a much more complex ESR hyperfine structure from dimer **2b** than from the corresponding 2-*p*-methylphenyl-4,5-diphenyl imidazole dimer (Fig. 6).

While the ESR signal of the lophine dimer in benzene is enhanced following UV irradiation (Fig. 7), the ESR signal of dimer **2b** in benzene becomes stronger on heating (Fig. 8). It is interesting to note that the ESR signal of dimer **2b** in the solid state is also enhanced on grinding (Fig. 9). These experiments confirm that the colored species obtained on UV

Fig. 10. Aromatic region of ^{1}H NMR spectrum of **2b** in $CDCl_3$.

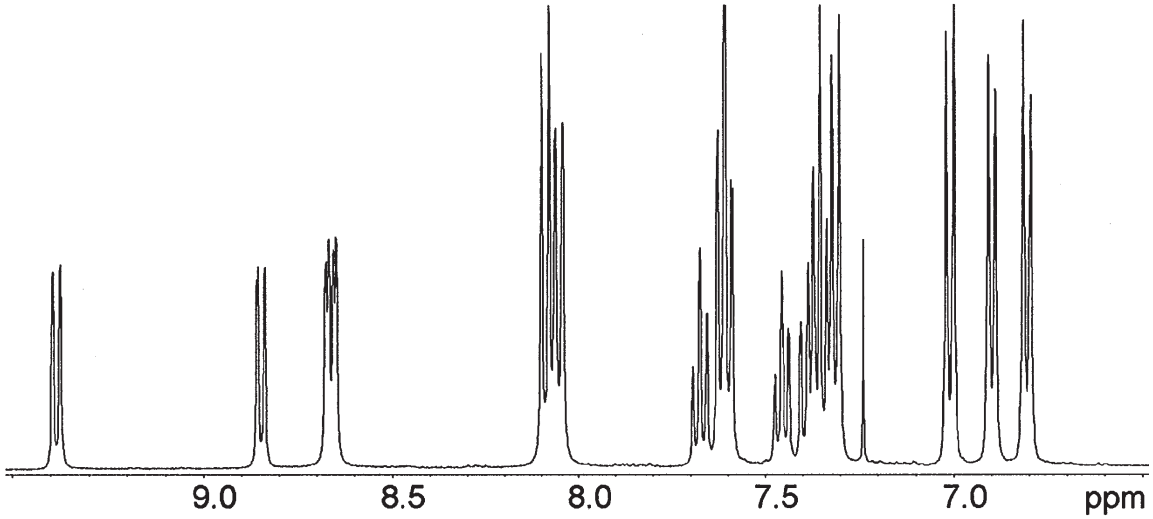

Table 6. MS data of dimers **2**.

	Melting point (lit.)	MS (*m*/*z*)
2a	200–203°C (8*a*)	(CI) 587.5(M^+), 295.3, 194.1
2b	170–173°C (8*a*)	(EI) 614.1(M^+), 308.1, 189.9, 163.0, 153.2, 82.8
2c		(EI) 642.2(M^+), 320.2, 189.8, 162.9, 116.8
2d		(EI) 636.1(M^+), 319.1, 189.8, 175.8, 162.6, 127.2, 116.8
2e		(EI) 646.4(M^+), 428.4, 324.3, 279.2, 235.2, 190.1, 176.0, 165.0, 149.0, 111.0
2f		(EI) 722.1(M^+), 362.1, 275.0, 198.7, 176.0, 162.6, 136.7, 128.6, 116.7
2g		(EI) 622.1(M^+), 312.1, 249.4, 235.9, 189.7, 175.8, 162.5,155.6, 130.8, 122.8, 116.7
2h	172–180°C (8*a*)	(EI) 654.1(M^+), 328.2, 189.9, 162.8, 136.9, 110.8
2i		(CI): 745.2(M^+), 667.3, 587.5, 373.3, 295.3, 194.1, 163.0

irradiation of the triphenylimidazole dimers, and also on heating the solutions of the phenanthroimidazole dimers or on grinding the phenanthroimidazole dimer, are free radical species. These qualitative observations on solutions of phenanthroimidazole dimers further validate the measurement of the molar extinction coefficient of the colored species as described above.

Experimental

The starting phenanthroimidazole compounds were synthesized according to the modification by Davidson et al. (23) of Radziszewski's imidazole synthesis (24). The dimers were synthesized by means of a two-phase reaction as described below.

To a solution of 1 g of the imidazole derivative in 250–350 mL methylene chloride was added a solution of potassium ferricyanide (5 g) and sodium hydroxide (5 g) in 100 mL water while cooling to 0°C and with vigorous stirring. The blue- or green-colored solution was stirred for 5 min at 0°C. The aqueous phase was separated and the organic phase was dried over sodium sulfate, and evaporated under reduced pressure to ca. 3 mL. After addition of ca. 3 mL ethyl acetate, the solution was placed in a refrigerator until crystals formed; these were filtered and washed with diethyl ether, yield over 90%. The MS data of the synthesized dimers are summarized in Table 6.

The UV–VIS spectroscopic measurements on the dimer solution in benzene were carried out by dissolution of ca. 20 mg of a dimer in 50 mL of benzene (BDH) freshly distilled from calcium hydride, followed by repetitive dilution to half concentration. UV–VIS spectra were recorded on an HP 8452A diode array spectrophotometer supported by HP89531A MS-DOS – UV–VIS operating software.The temperature of solutions in the cuvette (1 cm) was equilibrated to ± 0.1°C by means of a thermostatted water bath, RTE-210 (Neslab Instruments. Inc., Newington, NH 03801 U.S.A.). The UV light source for the irradiation was Spectroline, CX-Series (Spectronics Corporation, Westbury, New York).

NMR spectra were taken on a Bruker AM-400 NMR spectrometer operating at 400.134 MHz for ^{1}H and at 100.614 MHz for ^{13}C. The NMR solvents were purchased from CDN. The ESR spectra were recorded on a Varian E 104 ESR spectrometer and the UV light source for ESR measurement was a 1000-W Xe/Hg arc lamp. Sharp melting points could not be obtained; instead the sample in the capillary turned to a straw-colored resin-like material when the temperature was raised slowly (10°C/min). On raising the temperature quickly (>20°C/min) a transient blue or green color characteristic of the radical was observed; then the compound changed to the resin-like material. Purity was judged by the ^{1}H NMR spectra, which showed the absence of any extraneous peaks except for solvent (CH_2Cl_2 or EtOAc) of crystallization, which was difficult or impossible to remove, rendering

elemental analysis a poor criterion of purity. A typical ^{1}H NMR spectrum is shown in Fig. 10.

Acknowledgments

This research was supported by a grant from the Ontario Center for Materials Research. The authors are also grateful to Dr. L. Johnston, Dr. J. Lusztyk, and Dr. D. Shukla (National Research Council of Canada, Steacie Institute for Molecular Science) for assistance with the ESR measurements. We thank Prof. B.K. Hunter and Ms. S. Blake for helpful discussion on NMR data analysis.

References

1. H.C. van der Plas, M. Simonyi, F.C. Alderweireldt, and J.A. Lepoivre (*Editors*). Bio-organic heterocycles 1986. Elsevier, Amsterdam. 1986.
2. M. Patz, Y. Kuwahara, T. Suenobu, and S. Fukuzumi. Chem. Lett. 567 (1997).
3. T. Hayashi and K. Maeda. Bull. Chem. Soc. Jpn. **33**, 565 (1960).
4. T. Hayashi, K. Maeda, S. Shida, and K. Nakada. J. Chem. Phys. **32**, 1568 (1960).
5. (*a*) L.A. Cescon, G.R. Coraor, R. Dessauer, E.F. Silversmith, and E.J. Urban. J. Org. Chem. **36**, 2262 (1971); (*b*) B.S. Tanaseichuk, K.V. Stanovkina, A.N. Sunin, and L.G. Rezepova. Zh.Org. Khim. **5**, 2054 (1969); (*c*) B.S. Tanaseichuk and L.G. Rezepova. Zh. Org. Khim. **6**, 1065 (1970); (*d*) B.S. Tanaseichuk, A. A. Bardina, and V. A. Makskov. Zh. Org. Khim. 7, 1508 (1971). (*e*) B.S. Tanaseichuk, A.A. Bardina, and A.A. Khomenko. Khim. Geterotsikl. Soedin. **7**, 1255 (1971); (*f*) B.S. Tanaseichuk and S.V. Yartseva. Zh. Org. Khim. **7**, 1260 (1971); (*g*) Yu.A. Rozin, V.E. Blokhin, and Z.V. Pushreva. Khim. Geterotsikl. Soedin. **9**, 1105 (1973); (*h*) V.N. Shishkin, B.S. Tanashechuk, L.G. Tikhonova, and A.A. Bardina. Khim. Geterotsikl. Soedin. **9**, 387 (1973); (*i*) Yu.A. Rozin, V.E. Blokhin, Z.V. Pushreva, and V.I. Elin. Khim. Geterotsikl. Soedin. **10**, 990 (1974); (*j*) H. Baumgaertel and H. Zimmermann. Z. Naturforsch. B: Anorg. Chem. Org. Chem. Biochem. Biophys. Biol. **18B**, 406 (1961); (*k*) Chem. Ber. **99**, 843 (1966); (*l*) W. Suemmermann and H. Baumgaertel. Collect. Czech. Chem. Commun. **36**, 575 (1971); (*m*) Ber. Bunsen-Ges. Phys. Chem. **74**, 19 (1970).
6. (*a*) R.L. Mitchell, W.J. Nebe and W.M. Hardam. J. Imaging Sci. **30**, 215 (1986); (*b*) H.D. Hartzler (DuPont de Nemours & Co.). US Pat. 4,017,313 (1977); (*c*) Th.E. Duebner, B.M. Monroe (DuPont de Nemours & Co.). US Pat. 4,565,796 (1986); (*d*) H. Nagasaka (Mitsubishi Chem. Ind.). US Pat. 4,594,310 (1986).
7. L.A. Cescon, G.R. Coraor, R. Dessauer, A.S. Deutsch, H.L. Jackson, A. MacLachlan, K. Marcali, E.M. Potraftke, R.E. Read, E.F. Silversmith, and E.J. Urban. J. Org. Chem. **36**, 2267 (1971).
8. (*a*) Y. Sakaino, H. Kakisawa, and T. Kusumi. *J*. Chem. Soc. Perkin. Trans. 1, 2361 (1975); (*b*) J. Heterocycl. Chem. **12**, 953 (1975).
9. (*a*) B.M. Kosowski. CAMES sensor system, Plast. Technol. J. March, 1995; (*b*) A.C. Cordo and B.M. Kosowski. Int. Annu. Conf. ICT, 25th, 1994. p. 1; (*c*) D.C. Clark, W.E. Baker, A.C. Cordo, and B.M. Kosowski. Int. Polym. Process. Submitted; (*d*) D.C. Clark and W.E. Baker. Annu. Conf. Polym. Process. Soc. Secaucus, N.J. Paper 6, June 1997; (*e*) S.-R. Keum, S.-S. Hur, P.M. Kazmaier, and E. Buncel. Can. J. Chem. **69**, 1940 (1991); (*f*) S.-R. Keum, K.-B. Lee, P.M. Kazmaier, R.A. Manderville, and E. Buncel. Magn. Reson. Chem. **30**, 1128 (1992); (*g*) S.-R. Keum, K.-B. Lee, P.M. Kazmaier, and E. Buncel. Tetrahedron Lett. **35**, 1015 (1994); (*h*) S. Swansburg, Y.-K. Choi, S.-R. Keum, E. Buncel, and R.P. Lemieux. Liq. Cryst. **24**, 341 (1998); (*i*) S.-R. Keum,. M.J. Lee, S. Swansburg, E. Buncel, and R.P. Lemieux. Dyes Pigm. In press; (*j*) K.-S Cheon, R.A. Cox, S.-R. Keum, and E. Buncel. J. Chem. Soc. Perkin Trans. 2, 1231 (1998); (*k*) E. Buncel and K. -S Cheon. J. Chem. Soc. Perkin Trans. 2, 1241 (1998); (*l*) S.-R. Keum, P.M. Kazmaier, K.-S. Cheon. R.A. Manderville, and E. Buncel. Bull. Korean Chem. Soc. **17**, 391 (1996); (*m*) S.-R. Keum, S.S. Lim, B.H. Min, P.M. Kazmaier, and E. Buncel. Dyes Pigm. **30**, 225 (1996); (*n*) A. J. McKerrow, E. Buncel, and P.M. Kazmaier. Can. J. Chem. **73**, 1605 (1995); (*o*) E. Buncel, A.J. MacKerrow, and P.M. Kazmaier. J. Chem. Soc. Chem. Commun. 1242 (1992); (*p*) A.J. MacKerrow, E. Buncel, and P.M. Kazmaier. Can. J. Chem. **71**, 390 (1992); (*q*) P.M. Kazmaier, A.J. McKerrow, and E. Buncel. J. Imaging Sci. **36**, 373 (1992); (*r*) E. Buncel amd S. Rajagopal. Acc. Chem. Res. **23**, 226 (1990).
10. K. Maeda and T. Hayashi. Bull. Chem. Soc. Jpn. **43**, 429 (1970).
11. D.M. White and J. Sonnenberg. J. Am. Chem. Soc. **88**, 3825 (1966).
12. W.I. Talor and A.R. Battersby. Oxidative coupling of phenols. Marcel Dekker, Inc. New York. 1967.
13. D. Taub, C.H. Kuo, and N.L. Wendler. J. Org. Chem. **28**, 2752 (1963).
14. H. Tanino, T. Kondo, K. Okada, and T. Goto. Bull. Chem. Soc. Jpn. **45**, 1474 (1972).
15. J.D. Memory and N.K. Wilson. NMR of aromatic compounds. John Wiley &Sons, New York. 1982. p. 45.
16. D.H. Williams and I. Fleming. Spectroscopic methods in organic chemistry. 5th ed. McGraw–Hill Book Company, London. 1995. p. 112.
17. (*a*) Y. Sakaino, T. Takizawa, Y. Inouye, and H. Kakisawa. J. Chem. Soc. Perkin Trans. 2, 1623 (1986); (*b*) T. Hayashi, K. Maeda, and M. Morinaga. Bull. Chem. Soc. Jpn. **37**, 1563 (1964); (*c*) T. Hayashi, K. Maeda and T. Kanaji. Bull. Chem. Soc. Jpn. **38**, 857 (1965).
18. For pressure effects on organic compounds: (*a*) Z.A. Dreger and H.G. Drickamer. Chem. Phys. Lett. **179**, 199 (1991); (*b*) R.R. Birge, C.T. Berge, L.L. Noble, and R.C. Neuman, Jr. J. Am. Chem. Soc. **101**, 5162 (1979); (*c*) D.G. Wilson and H.G. Drickamer. J. Chem. Phys. 3649 (1975); (*d*) G. Kortuem and W. Zoller. Chem. Ber. **100**, 280 (1967); (*e*) S. Murphy. B. Sauerwein, H.G. Drickamer, and G.B. Schuster. J. Phys. Chem. **98**, 13476 (1994); (*f*) L. Comeford and E. Grunwald. J. Phys. Chem. **94**, 1105 (1990); (*g*) K. Song, R.D. Miller, and J.F. Rabolt. Macromolecules, **26**, 3232 (1993); (*h*) E. Orti, R. Crespo, and M.C. Piqueras. Synth. Met. **41**–**43**, 1575 (1991); (*i*) R.A. Nallicheri and M.F. Rubner. Macromolecules, **24**, 517 (1991). For pressure effects on metal complexes: (*j*) S. Alshehri, J. Burgess, G.H. Morgan, B. Patel, and M.S. Patel. Transition Met. Chem. (London), **18**, 619 (1993); (*k*) B. Scott and R.D. Willett. J. Am. Chem. Soc. **113**, 5253 (1991); (*l*) K.H. Drickamer and L. Bray. Acc. Chem. Res. **23**, 55 (1990); (*m*) M. Kotowski, R. van Edlik, R.B. Ali, J. Burgess, and S. Radulovic. Inorg. Chim. Acta, **131**, 225 (1987).
19. T.H. Lowry and K.S. Richardson. Mechanism and theory in organic chemistry. 3th ed. R.R. Donnelley & Sons, New York. 1987.
20. R.D. Allendoerfer and A.S. Pollock. Mol. Phys. **22**, 661(1971).
21. N. Cyr, M.A. Wilks, and M.R. Willis. J. Chem. Soc. B: 404 (1971).
22. H. Ueda. J. Phys. Chem. **68**, 1304 (1964).
23. D. Davidson, M. Weiss, and M. Jelling. J. Org. Chem. **2**, 319 (1937).
24. B. Radziszewski. Ber. Dtsch. Chem. Ges. **10**, 10 (1877).